Carbohydrate Polymers 99 (2014) 325–330

Contents lists available at ScienceDirect

Carbohydrate Polymers

journal homepage: www.elsevier.com/locate/carbpol

# Modeling of starch retrogradation onset in its aqueous solution using thermoreversible gelation concept

R. Nasseri, N. Mohammadi*

*Department of Polymer Engineering and Color Technology, Amirkabir University of Technology, P.O. Box 15875-4413, 424 Hafez Avenue, Tehran, Iran*

ARTICLE INFO

*Article history:*
Received 22 June 2013
Received in revised form 9 August 2013
Accepted 15 August 2013
Available online 20 August 2013

*Keywords:*
Helix distribution
Conformational loss
Double helix formation
Retrogradation
Starch aqueous solution

ABSTRACT

A model was developed to predict starch retrogradation onset in its aqueous solution and verified with the selected literature data. The most probable chain helix distribution was first estimated via minimizing the system free energy with respect to chain helix length. Later, the calculation was extended to double helix formation among single polymer chains with $\bar{\zeta}_2 = 10$ as the retrogradation criterion. $\bar{\zeta}_2$ is the average double helix length usually equals 10 implying the number of participating residues in the thickness of the thinnest reported starch lamella in the literature. The model prediction namely the retrogradation onset temperature, showed quite reasonable agreement with the selected literature data. Equal chain conformational entropy loss, $\Delta s/k_B \approx -0.7$, was inferred for various starch aqueous solutions due to the double helix kind of associations. Nonetheless, the studied systems showed distinct restrictions, $\sigma = 9 \times 10^{-4}$–$4.7 \times 10^{-3}$, against association.



## 1. Introduction

Starch is one of the most abundant, renewable, low cost and bio-degradable green polymer (Teixeira et al., 2009). It is mainly composed of two macromolecular components: linear amylose with α-1,4 linked glucan chain, and highly branched amylopectin with α-1,6 linkages joining linear chains (Yao, Zhang, & Ding, 2002). These macromolecules have been recently identified as high potential candidates for substituting various synthetic polymers (Monnet, Joly, Dole, & Bliard, 2010). Thermoplastic starch (TPS) is one the most important man-made products for replacement of synthetic polymers in certain applications. Starch processing into the plasticized one (TPS), involves some critical thermal transitions such as gelatinization and retrogradation (Shanks and Gunaratne, 2011). Gelatinization with water or other plasticizers occurs through hydrogen bonds disruption of starch granules via its swelling followed by melting leading to birefringence loss and solubilization (Perdon, Siebenmorgen, Buescher, & Gbur, 1999). Retrogradation, however, is nearly the reverse process dealing with structural transformation from an amorphous solution into the more ordered crystalline state (Tian, Xu, Xie, Zhao, & Jin, 2011). From molecular point of view, both linear amylose and branched amylopectin participate in the retrogradation process. Nonetheless, the former mainly experiences the early stage transition via an irreversible process, while the latter spends a longer retrogradation time due to its intrinsic molecular rigidity. Moreover, retrogradation of the amylopectin dictates the reversible starch gels rigidity and crystalline state (Iturriaga, Lopez de Mishima, & Añon, 2010). Therefore, amylopectin plays the most important role in starch property control through various thermal transitions. The retrogradation literature is mainly divided into two sub-divisions namely characterization techniques and modeling the phenomenon. It is worth mentioning that, most developed models emphasize on retrogradation kinetics rather than its thermodynamics using the classical or modified Avrami's equations (Del Nobile, Martoriello, Mocci, & La Notte, 2003).

Natural or synthetic linear polymers undergo a local conformational transition to all-trans or helix forms before their aggregation. The thermodynamics of junction formation by the helices has been adequately studied in several papers by Tanaka (2000, 2003) and Tanaka and Stockmayer (1994). Helix formation in amylopectin retrogradation, however, occurs in its side chains, complicating the phenomenon. Therefore, the Tanaka's model must be recapitulate briefly of the thermodynamic relation used for the quantitative description of association and extend them for investigating the retrogradation of starch. Accordingly, the retrogradation onset of starch aqueous solutions was predicted as a function of their solid content and validated with selected experimental data.

## 2. Theoretical work

In the gelatinization process or heating starch solution, the crystalline structure of biopolymer is disrupted followed by partial

* Corresponding author. Tel.: +98 2164542406; fax: +98 21645424.
*E-mail addresses:* rasool.nasseri@aut.ac.ir (R. Nasseri), mohamadi@aut.ac.ir (N. Mohammadi).

0144-8617/$ – see front matter © 2013 Elsevier Ltd. All rights reserved.
http://dx.doi.org/10.1016/j.carbpol.2013.08.028

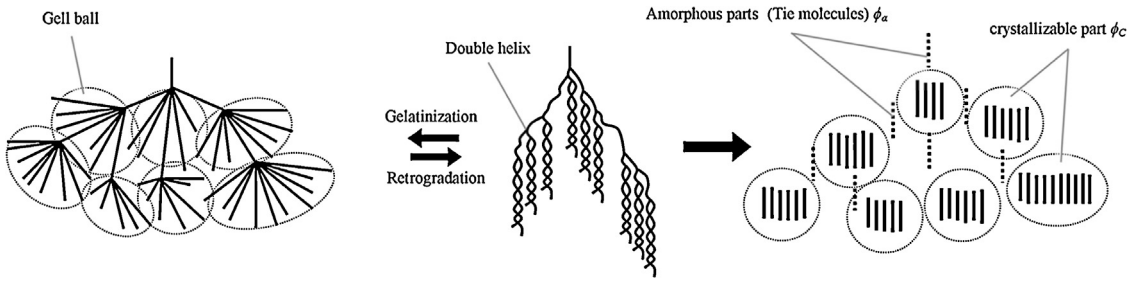


**Fig. 1.** Schematic representation of nano-structural evolution during gelatinization, retrogradation and the linearization of amylopectin molecule.

phase separation of amylose and amylopectine and gell ball formation in amylopectine short branches. By cooling the gelatinized amylopectin, however, the double-helical crystalline structures reform from their dissociated short-branches (Liu, Xie, Yu, Chen, & Li, 2009), Fig. 1. Theses double-helices contain at least ten residues or repeating units along their length (Le Corre, Bras, & Dufresne, 2010). Equally important, coil to helix transition is the prerequisite of double association in short branches of amylopectin molecules. Amylopectin treatment as an associative system requires its linearization besides application of the thermoreversible gelation concept. Accordingly, the associated chains of short amylopectin branches or backbones with 14–18 residues were treated distinctly as crystallizable short branches or tie molecules (Le Corre et al., 2010; Liu et al., 2009), Fig. 1.

The effect of solution concentration on its thermal transitions was considered using a lattice with $\Omega$ equal volume cells. The cells occupants are solvent molecules or same size repeat units of macromolecules. Therefore, the number of linear tie molecules forming the chain backbone is given by

$$N_\alpha = \frac{\Omega\varphi_\alpha}{n} \tag{1}$$

where $n$ is the number of hypothetical linear chains repeat units and $\varphi_\alpha$ is the volume fraction of the amorphous tie-molecules, Fig. 1.

$$\varphi_\alpha = \varphi(1 - C) = \varphi - \varphi_C \tag{2}$$

Here $C$ is the number fraction of crystallizable parts of amylopectin chains, which is replaced by the crystalline fraction of the sample. Linearized chain with suitable helix conformation takes part in crystal structure and extends to the nearly whole side chain length. Portions of a chain with helical conformation depict functional groups, while their lengths identify their group type (Tanaka, 2003). Chains are designated $\lambda$ and $\mu$ before and after helix formation acting as functional groups (Tanaka, 2000). Here, polymer chain is characterized only by the number of its functional groups for simplicity. This is not a drastic restriction and will be revised later on via differentiating among them in the final stage of modeling, Fig. 2.

The cluster of type $(\mathbf{j};\boldsymbol{l})$ is defined to consist $l_f$ primary molecules with functionality $f$ ($f = 0, 1, 2, 3, \ldots$) and $j_k$ junctions of multiplicity $k$ ($k = 1,2,3,\ldots$). The bold letters $\boldsymbol{l} \equiv \{l_0, l_1, l_2, l_3, \ldots\}$ and $\mathbf{j} \equiv \{j_1, j_2, j_3, \ldots\}$ are set of numbers that characterize the cluster type (Tanaka, 2000), Fig. 3.

If $N(\mathbf{j};\boldsymbol{l})$ is the number of $(\mathbf{j};\boldsymbol{l})$ clusters in the system (including $\lambda$, non-functional, and $\alpha$, amorphous linear parts of amylopectin molecules), then their number density would be:

$$\nu(\mathbf{j};\boldsymbol{l}) = \frac{N(\mathbf{j};\boldsymbol{l})}{\Omega} \tag{3}$$

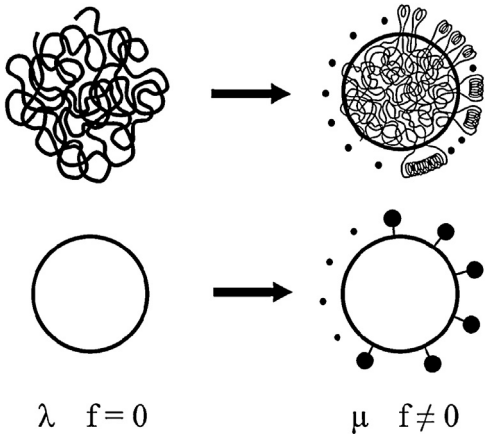


**Fig. 2.** Chain carrying different length helices is assumed a functional molecule; each helix corresponds with an indistinguishable functional group.

In addition, the volume fraction of clusters is

$$\varphi(\mathbf{j};\boldsymbol{l}) = \left(n\sum_{f\geq 0} l_f\right)\nu(\mathbf{j};\boldsymbol{l}) \tag{4}$$

The volume fraction of whole linearized chains is then given by

$$\varphi = \sum_{j,l}\varphi(\mathbf{j};\boldsymbol{l}) \tag{5}$$

The volume fraction of crystallizable chains can be calculated from its relationship with polymer volume fraction:

$$\varphi_C = C\varphi \tag{6}$$

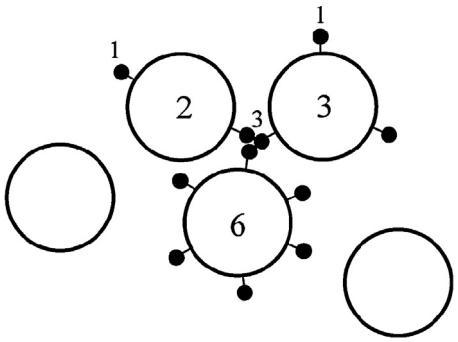


**Fig. 3.** Schematic representation of a cluster with tree functional ($\mu$) and two non-functional ($\lambda$ or $\alpha$) molecules.

If $N_f$ is the number of molecules with $f$ functional groups, then $\varphi$ equals:

$$\varphi = \frac{\sum_{f\geq 0} nN_f}{\Omega} \tag{7}$$

In the above equations, $f=0$ quantifies $\lambda$ and $\alpha$ molecules. Accordingly, their volume fractions are $\varphi_\lambda \equiv nN_\lambda/\Omega$ and $\varphi_\alpha \equiv nN_\alpha/\Omega$, respectively. Therefore, the volume fraction of $\mu$ molecules would be:

$$\varphi_\mu = \varphi - \varphi_\lambda - \varphi_\alpha = \frac{\sum_{f\geq 1} nN_f}{\Omega} \tag{8}$$

### 2.1. The free energy of amylopectin aqueous solution

The model system is composed of gel balls containing swelled amylopectin branches with water at temperature of $T$, and volume fraction of $\varphi$. The Flory–Huggins lattice theory is employed to calculate the system free energy (Flory, 1942; Huggins, 1942), while pure solvent and free branches imply the reference states. The free energy change between the reference states and the equilibrium final state containing clusters, has three major components (Tanaka, 2000)

$$\Delta F = \Delta F_{\text{conf}} + \Delta F_{\text{rea}} + \Delta F_{\text{mix}} \tag{9}$$

where $\Delta F_{\text{conf}}$, $\Delta F_{\text{rea}}$ and $\Delta F_{\text{mix}}$ are the free energy change due to the conformational change, the clusters formation, and the mixing of the clusters with water, respectively.

The conformational free energy change is written as

$$\Delta F_{\text{conf}} = A_\alpha N_\alpha + A_\lambda N_\lambda + \sum_{j,l}\left(\sum_{f\geq 1} A_f l_f\right) N(\mathbf{j};\boldsymbol{l}) + \sum_{f\geq 1} A_f N_f^{\text{C}} \tag{10}$$

where $N_\alpha$ and $N_\lambda$ are the number of $\alpha$-molecules and $\lambda$-molecules, respectively. $N_f^{\text{C}}$ is the number of $f$ functional molecules which participated in amylopectin crystals with the thinnest thickness. $A_\lambda$, $A_\alpha$ and $A_f$ are the conformational free energy of a single $\alpha$-molecule, $\lambda$-molecule and $\mu$-molecules with $f$ functional groups, respectively. The activation energy of functionalizing or forming helices in a molecule is accordingly:

$$\Delta A_f \equiv A_f - A_\lambda \tag{11}$$

The free energy change to form $N(\mathbf{j};\boldsymbol{l})$ clusters of type $(\mathbf{j};\boldsymbol{l})$ from the primary chains followed by crystallization via $N_f^{\text{C}}$ $f$ functional molecules will be

$$\beta\Delta F_{\text{rea}} = \sum_{j,l}\Delta(\mathbf{j};\boldsymbol{l})N(\mathbf{j};\boldsymbol{l}) + \sum_{f\geq 1}\delta_f(\varphi)N_f^{\text{C}} \tag{12}$$

where $\beta \equiv 1/k_{\text{B}}T$ and $k_{\text{B}}$ is the Boltzman constant and $\Delta(\mathbf{j};\boldsymbol{l})$ is the free energy of $(\mathbf{j};\boldsymbol{l})$ cluster formation from $\mu$ molecules in undiluted state (Tanaka, 2000):

$$\Delta(\mathbf{j};\boldsymbol{l}) \equiv \beta\{\mu^\circ(\mathbf{j};\boldsymbol{l}) - \sum_f l\mu^\circ(\mathbf{j}_{0f};\boldsymbol{l}_{0f})\} \tag{13}$$

The superscript designates the undiluted state. The second term at the right hand side of Eq. (12) appears only when some of helices form crystalline regions. $\delta_f$ is the free energy change due to joining a $f$ molecule to the crystal. Since the degree of association increases with polymer concentration, $\delta_f$ is assumed concentration dependent. Finally, the last term of Eq. (9) implies the free energychange of mixing clusters with water. According to the Flory–Huggins theory, the mixing energy can be written as:

$$\beta\Delta F_{\text{mix}} = N_0 \ln\varphi_0 + N_\lambda \ln\varphi_\lambda + N_\alpha \ln\varphi_\alpha + \sum_{j,l} N(\mathbf{j};\boldsymbol{l})\ln\varphi(\mathbf{j};\boldsymbol{l}) + \Omega\chi\varphi_0\varphi \tag{14}$$

where $\chi$ is the Flory's interaction parameter. The chemical potentials of the components are required as the prerequisite of the free energy calculation. The chemical potential of each component is the derivative of the system free energy with respect to the number of that component

$$\beta\Delta\mu_0 = \ln\varphi_0 + \varphi - \sum_{j,l}\nu(\mathbf{j};\boldsymbol{l}) + \chi\varphi^2 - [\sum_f \delta_f'(\varphi_{\text{C}})\nu_f^{\text{C}}]\varphi C - \frac{(1-C)}{n}\varphi \tag{15}$$

$$\frac{\beta\Delta\mu_\lambda}{n} = \frac{1+\ln\varphi_\lambda + \beta A_\lambda}{n} - 1 + \varphi - \sum_{j,l}\nu(\mathbf{j};\boldsymbol{l}) + \chi\varphi_0^2 + [\sum_f \delta_f'(\varphi_{\text{C}})\nu_f^{\text{C}}]\varphi_0 C + \frac{(1-C)}{n}\varphi_0 \tag{16}$$

$$\frac{\beta\Delta\mu_\alpha}{n} = \frac{1+\ln\varphi_\alpha + (1-C)\varphi_0 + \beta A_\alpha}{n} - \varphi_0 - \sum_{j,l}\nu(\mathbf{j};\boldsymbol{l}) + \chi\varphi_0^2 + [\sum_f \delta_f'(\varphi_{\text{C}})\nu_f^{\text{C}}]\varphi_0 C \tag{17}$$

Then, free energy density of the system equals:

$$\frac{\beta\Delta F}{\Omega} = \beta\Delta\mu_0\varphi_0 + \beta\frac{\Delta\mu_\lambda}{n}\varphi_{\text{C}} + \beta\frac{\Delta\mu_\alpha}{n}\varphi_\alpha \tag{18}$$

$\alpha$ and $\lambda$ define the reference states of polymer chains so that $A_\alpha$ and $A_\lambda$ equal zero. Then the free energy density of the system can be calculated using Eq. (19).

$$\frac{\beta\Delta F}{\Omega} = f_{\text{FH}}(\varphi) + f_{\text{AS}}(\varphi) \tag{19}$$

where $f_{\text{FH}}$ and $f_{\text{AS}}$ are the mixing and association free energies, respectively:

$$f_{\text{FH}}(\varphi) = \frac{\varphi_{\text{C}}}{n}\ln\varphi_{\text{C}} + \frac{\varphi_\alpha}{n}\ln\varphi_\alpha + (1-\varphi) + \chi\varphi(1-\varphi) \tag{20}$$

and

$$f_{\text{AS}}(\varphi) = \frac{\varphi_{\text{C}}}{n}\ln\left(\frac{\varphi_\lambda}{\varphi_{\text{C}}}\right) + \frac{\varphi}{n} - \sum_{j,l}\nu(\mathbf{j};\boldsymbol{l}) \tag{21}$$

The functional groups (helices) are now differentiated by the number of their repeat units. If $j_\zeta$ is the number of helices with the lengths of $\zeta = 1, 2, 3, \ldots, n$, the number of different ways to select $j \equiv \{j_1, j_2, j_3, \ldots\}$ is the chain helix distribution. Then, free energy can be minimized with respect to this parameter. The number of different ways to select $j$ is the most important variable, which is computed by combinatorial counting method (Tanaka, 2003):

$$\omega(\{j\}) = \frac{(n - \sum \zeta j_\zeta)!}{(\prod j_\zeta!)(n - \sum \zeta j_\zeta - \sum j_\zeta)!} \tag{22}$$

For the double helix case, however, the second and third components of the association part of free energy density can be replaced by

$$\frac{\varphi}{n} - \sum_{j,l} \nu(\mathbf{j};\boldsymbol{l}) = \sum_{\zeta} \frac{1}{\lambda_\zeta} \int_0^{z_\zeta} z dz \tag{23}$$

where the temperature dependent $\lambda_\zeta(T)$ is the association constant, which indicates the probability of helices with length of $\zeta$ to bound into a junction. According to the Zimm–Bragg gelation model (Zimm & Bragg, 1959), the association constant is written as:

$$\lambda_\zeta = \sigma\lambda(T)^\zeta \tag{24}$$

where $\sigma$ is the probability of an arbitrarily chosen pair of monomers on different chains start winding. In inter-monomer winding without restriction, $\sigma$ equals unity. On the other hand, $\lambda(T)$ correlates with the hydrogen bond formation probability between two monomers of a helix and can be estimated in terms of the entropy and enthalpy of association:

$$\ln\ \lambda(T) = \frac{\Delta S}{K_B} - \frac{\varepsilon_A}{K_B T} \tag{25}$$

The activation energy with the enthalpic character ($|\varepsilon_A|$) can be then estimated as the average hydrogen bond formation energy between a hydroxyl group and oxygen (22 kJ/mol (Curtiss & Blander, 1988)) of two starch residues. The chain un-reacted groups, $z_\zeta$, in Eq. (23) is calculated using the volume fraction of crystallizable polymer sactions:

$$\frac{\lambda_\zeta j_\zeta \varphi_C}{n} = z_\zeta^2 \tag{26}$$

By substituting Eq. (23) in Eq. (21), the association part of the system free energy can be written as

$$f_{AS}(\varphi) = \frac{\varphi_C}{n} \ln\left(\frac{\varphi_\lambda}{\varphi_C}\right) + \sum_{\zeta} \frac{1}{\lambda_\zeta} \int_0^{z_\zeta} z dz \tag{27}$$

The volume fraction of λ molecules correlates to the volume fraction of crystallizable parts as:

$$\frac{\varphi_\lambda}{\varphi_C} = \frac{1}{F(\{z\})} \tag{28}$$

where the $F$ function will be

$$F(\{z\}) \equiv \sum_{j\neq 0} \prod_{\zeta} [z_\zeta^{j_\zeta}] \omega(\{j\}) \tag{29}$$

### 2.2. The minimization of free energy density

The helix distribution function of a system with specific volume fraction and temperature, can be calculated via its free energy minimization, $\partial(\beta\Delta F/\Omega)/\partial j_\zeta = 0$. The solution leads to double helix distribution function as:

$$\frac{j_\zeta}{n} = (1-\theta)^2 t^2 \varphi_C \lambda_\zeta (t^2)^\zeta \tag{30}$$

$t$ is the probability of an arbitrarily chosen monomer to be in the random coil part of the linearized chains and is defined by

$$t \equiv \frac{(1-\theta-\nu)}{(1-\theta)} \tag{31}$$

where $\theta$ and $\nu$ are double helix content and normalized number of repeat units of the double helices, respectively:

$$\theta \equiv \frac{\sum_{\zeta=1}^{n} \zeta j_\zeta}{n} \tag{32}$$

$$\nu \equiv \frac{\sum_{\zeta=1}^{n} j_\zeta}{n} \tag{33}$$

For double helix association, these parameters are simplified as:

$$\theta = (1-\theta)^2 t^2 \varphi_C W_1^{(2)}(t^2) \tag{34}$$

$$\nu = (1-\theta)^2 t^2 \varphi_C W_0^{(2)}(t^2) \tag{35}$$

where $W$s are defined as (Tanaka, 2003)

$$W_0^{(2)}(t^2) = \sigma^2 \lambda t^2 w_0(\lambda t^2) \tag{36}$$

$$W_1{}^{(2)}(t^2) = \sigma^2 \lambda t^2 w_1(\lambda t^2) \tag{37}$$

while

$$w_0(x) \equiv \sum_{\zeta=1}^{n} x^{\zeta-1} \tag{38}$$

$$w_1(x) \equiv \sum_{\zeta=1}^{n} \zeta x^{\zeta-1} \tag{39}$$

The $t$ parameter can be then calculated using the following equation

$$(1-t)\left\{1 + \frac{w_1(\lambda t^2)(1-t)}{w_0(\lambda t^2)}\right\} = \sigma\lambda\varphi_C t^4 w_0(\lambda t^2) \tag{40}$$

Finally, the average length of double helices ($\bar{\zeta}_2$) can be calculated by dividing double helix content to their normalized number of repeat units

$$\bar{\zeta}_2 = \frac{\theta}{\nu} = \frac{W_1^{(2)}(t^2)}{W_0^{(2)}(t^2)} \tag{41}$$

By substituting Eqs. (36) and (37) in Eq. (41) and using Eqs. (25), (38) and (39) then taking $n = 16$ as the length of linearized chains, $\bar{\zeta}_2$ can be calculated as a function of temperature with the following equation

$$\bar{\zeta}_2 = \sum_{M=1}^{16} M \left[\sum_{\zeta=1}^{16} \exp\left[(\zeta - M)\left(\frac{\Delta S}{K_B} - \frac{\varepsilon_A}{K_B T}\right)\right] t^{2(\zeta-M)}\right]^{-1} \tag{42}$$

### 2.3. Model validation

The type, amylopectin content, the percentage of crystallinity and aging condition of selected starches after gelatinization were extracted and tabulated, Table 1 (Avérous, Fringant, & Moro, 2001; Kim, Kim, & Shin, 1997; Zeleznak & Hoseney, 1986; Zhou, Baik, Wang, & Lim, 2010). The retrogradation onset was reported explicitly or extracted from the DSC thermographs of the aged aqueous starch solutions. $\sigma$ and $\Delta s/k_B$ of different samples were obtained from fitting the experimental data on the model predictions. For the fitting procedure, at first, initial values for $\sigma$ and $\Delta s/K_B$ were estimated and λ was calculated using Eq. (25). Then, for concentrations in which experimental onset temperatures were existed t was calculated with reciprocal Eq. (40). In the next step, temperature dependency of $\bar{\zeta}_2$ can be obtained by Eq. (42) and by taking $\bar{\zeta}_2 = 10$ as the criterion, retrogradation onset temperatures can be calculated and compared with experimental data points. Then, iteration process was continued by amendment of the initial estimations of $\sigma$ and $\Delta s/k_B$ until the difference between calculated and experimental temperatures became minimized, Fig. 4. $\Delta s/K_B$ of the selected samples from several research works were about −0.7. Therefore, similar conformational loss is expected for two adjacent repeat

**Table 1**
The type, amylopectin content and the percent of crystallinity of selected starches and their aging conditions, $\sigma$ and $\Delta s/k_B$.

| Starch type | Amylopetin content (%) | Crystallinity (%) | Aging condition | $\Delta s/K_B$ | $\sigma$ | Reference |
|---|---|---|---|---|---|---|
| Waxy corn | 100 | 31[b] | One day at 7 °C and one day at 30 °C intermittently for seven days | −0.7324 | 0.0047 | Zhou et al. (2010) |
| Wheat | 83[a] | 36[a] | Seven days at 25 °C | −0.7173 | 0.0024 | Zeleznak and Hoseney (1986) |
| Waxy maize | 98.4 | 39[a] | Seven days at 6 °C | −0.7644 | 0.0011 | Avérous et al. (2001) |
| Waxy rice | 99.3 | 45[a] | Three days at 18 °C | −0.7623 | 0.0009 | Kim et al. (1997) |

[a] Le Corre et al. (2010).
[b] Chen and Evans (2005).

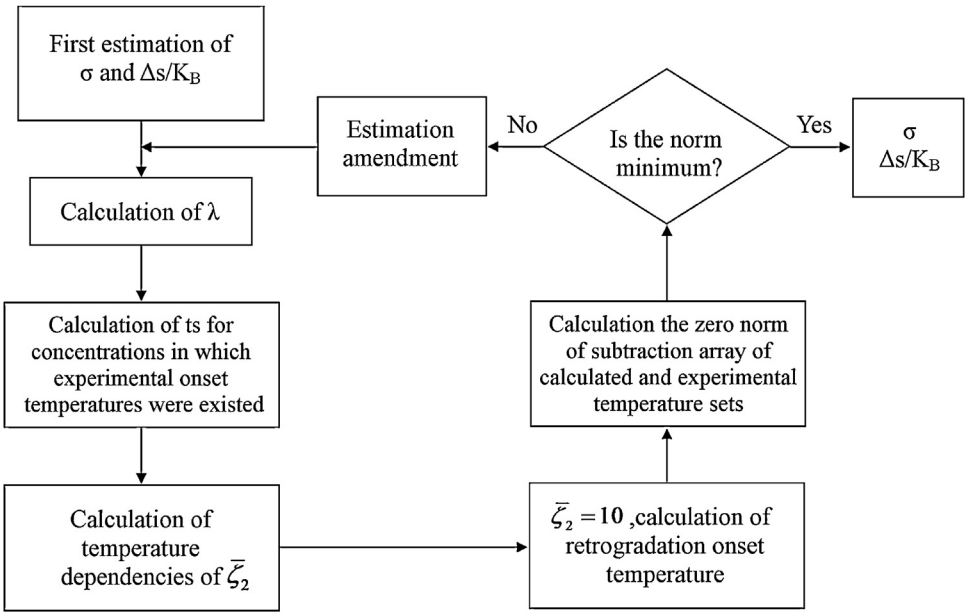


**Fig. 4.** Flowchart of iterative fitting algorithm.

units due to forming hydrogen bonds. However, the calculated $\sigma$s were quite different from $9 \times 10^{-4}$ up to $4.7 \times 10^{-3}$ which implies distinct restrictions against double helix formation. The effective parameter depends on the amylopectin branching content, type, size and branch distribution.

The average length of double helices versus the temperature of wheat starch aqueous solution is shown in Fig. 5. The retrogradation criterion was selected 10 and showed with a horizontal dash line. Therefore, the retrogradation onset was determined as the dash line intercept with various curves.

The retrogradation onset loses its sensitivity by the starch solution concentration increase. The plot of retrogradation onset versus the volume fraction of different starch aqueous solutions delineated reliable model predictions in comparison with the experimental results, Fig. 6.

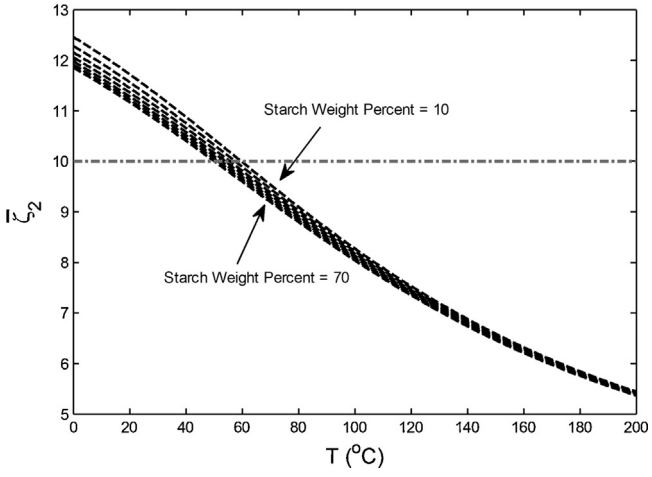


**Fig. 5.** Typical average lengths of double helices versus temperature for wheat sample, $\sigma$ is 0.0024 and $\Delta s/k_B$ is −0.7173. Weight percent of starch in its aqueous solution varies from curve to curve.

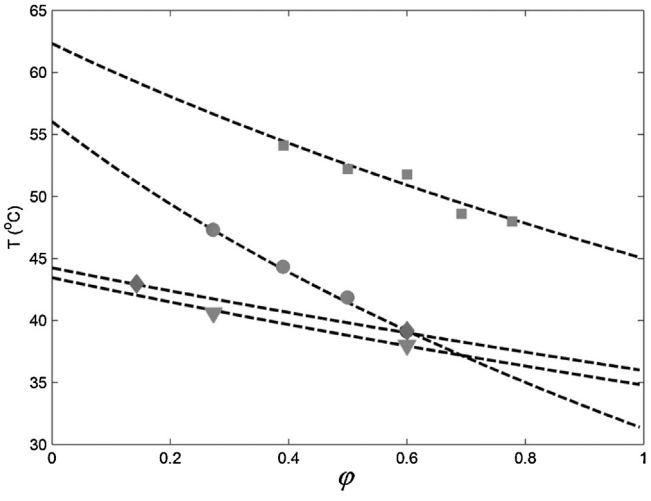


**Fig. 6.** Retrogradation onset temperature versus concentration for several samples: (●) waxy corn, (■) wheat, (▼) waxy maize and (♦) waxy rice. The dashed curves are the model predictions.

It is worth mentioning that data points are limited in certain cases for generalizing the model reliability. Nevertheless, the predicted trends of experimental data were satisfactory. In addition, model predictions regarding the retrogradation onset close to the neat solvent or very concentrated starch solutions are subjective. Physically, in low volume fraction starch solutions, the retrogradation would not be feasible due to the requirement of crossing the threshold concentration for any association. On the other hand, gelatinization and retrogradation of highly viscous starch solutions are forbidden kinetically (Zeleznak & Hoseney, 1986).

## 3. Conclusions

A model was developed to predict the retrogradation onset of starch solutions via using thermoreversible gelation concept. The calculated most probable helix distribution of linearized amylopectin chains via free energy minimization with respect to helix length led to the probability of double helix formation. Accordingly, the double helix length of the thinnest amylopectin crystals was chosen as the retrogradation criterion. The model predictions were compared with several selected experimental data point from literature. While, the entropy change due to hydrogen bond formation between two adjacent residues for different starch types were identical, relatively large differences was detected for $\sigma$ due to distinct restrictions against double helix formation.

## References


Avérous, L., Fringant, C., & Moro, L. (2001). Starch-based biodegradable materials suitable for thermoforming packaging. *Starch-Stärke*, *53*, 368–371.

Chen, B., & Evans, J. R. G. (2005). Thermoplastic starch-clay nanocomposites and their characteristics. *Carbohydrate Polymers*, *61*, 455–463.

Curtiss, L., & Blander, M. (1988). Thermodynamic properties of gas-phase hydrogen-bonded complexes. *Chemical Reviews*, *88*, 827–841.

Del Nobile, M., Martoriello, T., Mocci, G., & La Notte, E. (2003). Modeling the starch retrogradation kinetic of durum wheat bread. *Journal of Food Engineering*, *59*, 123–128.

Flory, P. J. (1942). Thermodynamics of high polymer solutions. *The Journal of Chemical Physics*, *10*, 51–61.

Huggins, M. L. (1942). Some Properties of Solutions of Long-chain Compounds. *The Journal of Physical Chemistry*, *46*, 151–158.

Iturriaga, L. B., Lopez de Mishima, B., & Añon, M. C. (2010). A study of the retrogradation process in five argentine rice starches. *LWT-Food Science and Technology*, *43*, 670–674.

Kim, J. O., Kim, W. S., & Shin, M. S. (1997). A comparative study on retrogradation of rice starch gels by DSC, X-ray and α-amylase methods. *Starch-Stärke*, *49*, 71–75.

Le Corre, D., Bras, J., & Dufresne, A. (2010). Starch nanoparticles: A review. *Biomacromolecules*, *11*, 1139–1153.

Liu, H., Xie, F., Yu, L., Chen, L., & Li, L. (2009). Thermal processing of starch-based polymers. *Progress in Polymer Science*, *34*, 1348–1368.

Monnet, D., Joly, C., Dole, P., & Bliard, C. (2010). Enhanced mechanical properties of partially beta-amylase trimmed starch for material applications. *Carbohydrate Polymers*, *80*, 747–752.

Perdon, A., Siebenmorgen, T., Buescher, R., & Gbur, E. (1999). Starch retrogradation and texture of cooked milled rice during storage. *Journal of Food Science*, *64*, 828–832.

Shanks, R. A., & Gunaratne, L. M. W. K. (2011). Gelatinization and retrogradation of thermoplastic starch characterized using modulated temperature differential scanning calorimetry. *Journal of Thermal Analysis and Calorimetry*, *106*(1), 93–99.

Tanaka, F. (2000). Thermoreversible gelation strongly coupled to polymer conformational transition. *Macromolecules*, *33*, 4249–4263.

Tanaka, F. (2003). Thermoreversible gelation driven by coil-to-helix transition of polymers. *Macromolecules*, *36*, 5392–5405.

Tanaka, F., & Stockmayer, W. H. (1994). Thermoreversible gelation with junctions of variable multiplicity. *Macromolecules*, *27*, 3943–3954.

Teixeira, E. d. M., Pasquini, D., Curvelo, A. A. S., Corradini, E., Belgacem, M. N., & Dufresne, A. (2009). Cassava bagasse cellulose nanofibrils reinforced thermoplastic cassava starch. *Carbohydrate Polymers*, *78*, 422–431.

Tian, Y., Xu, X., Xie, Z., Zhao, J., & Jin, Z. (2011). Starch retrogradation determined by differential thermal analysis (DTA). *Food Hydrocolloids*, *25*(6), 1637–1639.

Yao, Y., Zhang, J., & Ding, X. (2002). Structure-retrogradation relationship of rice starch in purified starches and cooked rice grains: A statistical investigation. *Journal of Agricultural and Food Chemistry*, *50*, 7420–7425.

Zeleznak, K., & Hoseney, R. (1986). The role of water in the retrogradation of wheat starch gels and bread crumb. *Cereal Chemistry*, *63*, 407–411.

Zhou, X., Baik, B. K., Wang, R., & Lim, S. T. (2010). Retrogradation of waxy and normal corn starch gels by temperature cycling. *Journal of Cereal Science*, *51*, 57–65.

Zimm, B. H., & Bragg, J. (1959). Theory of the phase transition between helix and random coil in polypeptide chains. *The Journal of Chemical Physics*, *31*, 526–535.